Pergamon

Scripta Materialia, Vol. 34, No. 11, pp. 1771–1777, 1996
Elsevier Science Ltd

1359-6462/96 $12.00 + .00

PII S1359-6462(96)00046-2

ON THE CRITICAL CONDITIONS OF KINK BAND FORMATION IN FIBER COMPOSITES WITH DUCTILE MATRIX

Ming Dao and Robert J. Asaro
Department of Applied Mechanics and Engineering Sciences, 0411
University of California, San Diego, La Jolla, CA 92093, USA

(Received October 18, 1995)
(Revised January 10, 1996)

Introduction

Fiber reinforced composites are used in an increasing number of structural applications, this due to their higher strength and stiffness to weight ratios as compared to monolithic structural materials. However, whereas fiber reinforced composites have high tensile strengths along the fiber directions, only about 50-60% of their tensile strengths can be achieved under compression [1, 2]. It is, therefore, important to understand the failure/damage modes under compressive loading.

The failure modes for unidirectional fiber composites under compressive loading display four mechanisms (Jelf and Fleck [3]): i) fiber buckling with elastic matrix deformation; ii) fiber crushing by yielding of the fiber or fiber splitting; iii) failure of the matrix; and iv) kink band formation. Among the four failure modes, kink band formation is believed to be the more important failure mode for modern structural composite materials, especially for those with ductile matrices (see *e.g.* Jelf and Fleck [3] for a detailed discussion).

It is fairly well established that kink band formation, in particular, the compressive strength of the composite, is controlled by fiber misalignment and the shear yield strength of the matrix (see *e.g.* Argon [4], Budiansky [5], Jelf and Fleck [3], Budiansky and Fleck [1], Kyriakides, Arseculeratne, Perry and Liechti [2], Moran, Liu and Shih [6]). The study of kink band formation in fiber composites has received a great deal of attention in the past 15 years. However, there are two important issues regarding the critical conditions for kink band formation that require further understanding:

1) It is experimentally verified that, under uniaxial compression, critical loading stress σ_C can be expressed as

$$\sigma_C = \frac{\tau_Y}{\sin\bar{\phi}\cos\bar{\phi}} \approx \frac{\tau_Y}{\bar{\phi}}, \tag{1}$$

where τ_Y is the critical resolved shear stress along fiber direction, and $\bar{\phi}$ is an effective imperfection tilt angle. Equation (1), however, is actually a yield criterion for the composite with an effective imperfection tilt angle $\bar{\phi}$. The question is therefore: why can the composite yield stress be used as the critical loading stress for kink band formation.

2) While a good criterion, *viz.* equation (1), has been experimentally established for the compressive strength of fiber composites, a more accurate method to predict kink band angles is still missing.

The purpose of this study was, therefore, to establish a general constitutive framework, and to address the aforementioned fundamental issues regarding kink band formation.

The Constitutive Theory

As pointed out by others [4, 5, 1], shear yielding along the fiber directions is the major deformation mode for unidirectional fiber composites, especially under compressive loading. Recently, Moran, Liu and Shih [6] used a "homogenized" simple slip (shear) model to describe the plastic deformation in fiber composites. We use the same concept in developing our constitutive framework. Figure 1(a) shows that, the dominating plastic deformation mode in unidirectional fiber composites is shear deformation along fiber direction; Figure 1(b) shows the deformation mode for a single crystal undergoing single slip, where shear (slip) deformation along the slip direction is the only plastic deformation mode. Both deformation modes in Figure 1 are analogous to the co-operative "deformation" of a deck of cards. Since the fiber spacing is far smaller than the structure size, the composite material can be treated as "homogenized". The plastic deformation mode in our homogenized fiber composite model is exactly the same as that in a single crystal undergoing single slip as noted in Figure 1, as long as the fibers are identified with the crystal's lattice slip planes. Similarly, the elastic properties of the fiber composite are treated as composite aggregate values instead of separated fiber and matrix values.

The constitutive law can be written in a form similar to that developed by Hill and Rice [7], Asaro and Rice [8] and Asaro [9], which is based on the work of Taylor [10]. The constitutive framework has been applied and extended to study localized deformation modes in single crystals, *e.g.* Peirce, Asaro and Needleman [11, 12] and more recently Dao and Asaro [13, 14, 15, 16].

Similar to the slip system in single crystals, we first introduce the shearing along the fiber direction as the composite slip system, which is defined by orthogonal unit vectors **s** and **m**, where **s** is the current fiber (slip) direction and **m** is normal to the slip plane. The total deformation rate, **D**, and spin rate, Ω, are composed by two parts. The first part is the plastic part, where the material deforms by shearing along the slip system (fiber direction) of the composite; the plastic deformation rate $\mathbf{D}^P$ and the plastic spin rate Ω^P are given by

$$\mathbf{D}^P = \mathbf{P}\dot{\gamma} \quad \text{and} \quad \Omega^P = \mathbf{W}\dot{\gamma}\,, \tag{2}$$

respectively, where $\dot{\gamma}$ is the shearing rate of the slip system, and

$$\mathbf{P} = \frac{1}{2}(\mathbf{sm} + \mathbf{ms}) \quad \text{and} \quad \mathbf{W} = \frac{1}{2}(\mathbf{sm} - \mathbf{ms})\,. \tag{3}$$

The second part is the elastic plus the rigid body rotation part, where material deforms by elastic deformation and the rigid body rotations; this part of deformation rate and spin rate are denoted by $\mathbf{D}^*$ and Ω^* respectively. Thus we can add the two parts together to obtain

$$\mathbf{D} = \mathbf{D}^* + \mathbf{P}\dot{\gamma} \quad \text{and} \quad \Omega = \Omega^* + \mathbf{W}\dot{\gamma}. \tag{4}$$

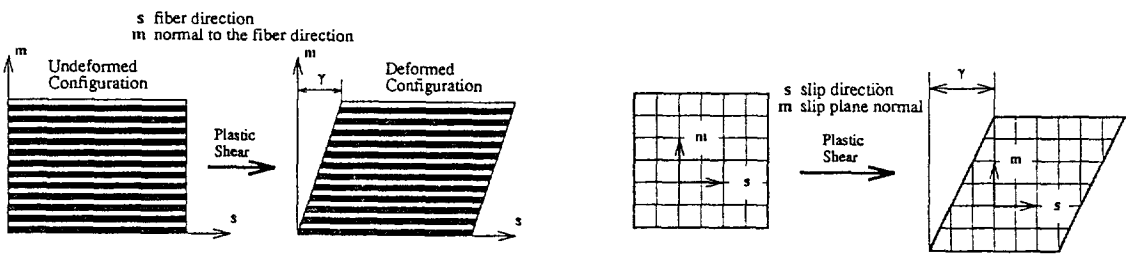

(a) Unidirectional fiber composite

(b) Single crystal under the single slip deformation mode

Figure 1. (a) The dominating plastic deformation mode in an unidirectional fiber composite is shear deformation along fiber direction, the deformation is assumed to be plane strain for simplicity; (b) the deformation mode for a single crystal undergoing single slip, where shear (slip) deformation along the slip direction is the only plastic deformation mode. Both deformation modes in the figure are analogous to the co-operative "deformation" of a deck of cards.

The material yield criterion is taken to be the Schmid rule, *i.e.*

$$\tau = \mathbf{m} \cdot \boldsymbol{\sigma} \cdot \mathbf{s} = \tau_Y \,, \tag{5}$$

where τ is the current value of the resolved shear stress, $\boldsymbol{\sigma}$ is the Cauchy stress tensor, and τ_Y is the current shear resistance. If the slip system is to remain active, taking derivatives of both sides of (5) with respect to time t, we must have

$$\dot{\tau} = h\dot{\gamma} \,, \tag{6}$$

where h is the shear strain hardening moduli. Following the procedure found in Asaro and Rice [8] and Asaro [9], we have the final constitutive equation

$$\overset{\nabla}{\boldsymbol{\sigma}} + \boldsymbol{\sigma} tr(\mathbf{D}) = \left\{ \mathbf{L} - \frac{1}{h + \mathbf{P} : \mathbf{L} : \mathbf{P}} (\mathbf{L} : \hat{\mathbf{P}})(\mathbf{P} : \mathbf{L}) \right\} : \mathbf{D} \,, \tag{7}$$

where $\mathbf{L}$ is the elastic moduli, and $\hat{\mathbf{P}} = \mathbf{P} + \mathbf{L}^{-1} : (\mathbf{W} \cdot \boldsymbol{\sigma} - \boldsymbol{\sigma} \cdot \mathbf{W})$.

Critical Conditions of Kink Band Formation

For materials described by idealized rate-independent constitutive laws Hill [17] has given a general theory of bifurcation of a homogeneous elastic-plastic flow field into bands of localized deformation. For this to occur there is first the kinematical restriction that for localization in a thin planar band with unit normal $\mathbf{n}$ (see Figure 2) the velocity gradient field inside the band $\partial \mathbf{v}/\partial \mathbf{x}$ can differ from that outside, $\partial \mathbf{v}^0/\partial \mathbf{x}$, as

$$\frac{\partial \mathbf{v}}{\partial \mathbf{x}} - \frac{\partial \mathbf{v}^0}{\partial \mathbf{x}} = \mathbf{g}\mathbf{n} \,. \tag{8}$$

In addition, there is the continuing equilibrium requirement that

$$\mathbf{n} \cdot \dot{\boldsymbol{\sigma}} - \mathbf{n} \cdot \dot{\boldsymbol{\sigma}}^0 = \mathbf{0} \tag{9}$$

at incipient localization where $\dot{\boldsymbol{\sigma}}$ is the stress rate inside the band and $\dot{\boldsymbol{\sigma}}^0$ that outside.

Constitutive law (7) along with the conditions for localization (8) and (9) can be solved to obtain critical conditions for the onset of localization. Following the procedure in Asaro and Rice [8], the critical condition of localization on a plane of normal $\mathbf{n}$ can be expressed as

$$-h - \mathbf{P} : \mathbf{L} : \mathbf{P} + (\mathbf{P} : \mathbf{L} \cdot \mathbf{n}) \cdot [\mathbf{I} + (\mathbf{n} \cdot \mathbf{L} \cdot \mathbf{n})^{-1} \cdot \mathbf{A}]^{-1} \cdot (\mathbf{n} \cdot \mathbf{L} \cdot \mathbf{n})^{-1} \cdot (\mathbf{n} \cdot \mathbf{L} : \hat{\mathbf{P}}) = 0 \,, \tag{10a}$$

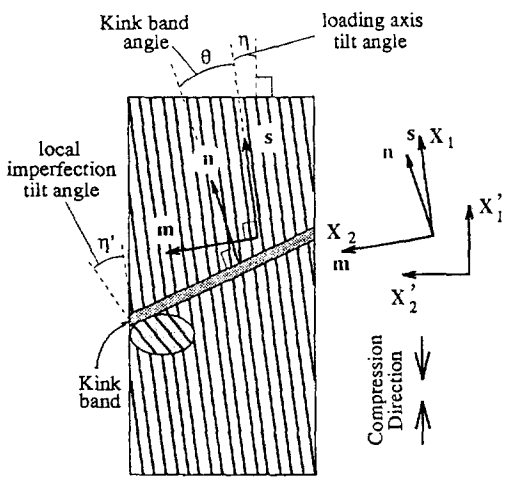

Figure 2. The geometry of a unidirection fiber composite with a kink band. Angle θ is the angle between the kink band normal $\mathbf{n}$ and the fiber direction $\mathbf{s}$, angle η is the loading axis tilt angle, and angle η' is the local imperfection tilt angle.

where

$$\mathbf{A} = \frac{1}{2}\{(\mathbf{n}\cdot\mathbf{L}\cdot\mathbf{n})\mathbf{I} - \boldsymbol{\sigma} - (\mathbf{n}\cdot\boldsymbol{\sigma})\mathbf{n} - \mathbf{n}(\boldsymbol{\sigma}\cdot\mathbf{n})\} \tag{10b}$$

with $\mathbf{I}$ the second order unit tensor.

Solution for Kink Band

As discussed by Asaro and Rice [8], two types of solutions can be found, *i.e.* shear bands that are almost parallel to the active slip planes and shear bands that are almost perpendicular to the active slip planes. Here we will be focusing on kink band formation. We seek solutions for kink bands, or solutions with the normal to the kink band $\mathbf{n}$ close to the slip direction $\mathbf{s}$, *i.e.* $\mathbf{n} = \mathbf{s} + \boldsymbol{\epsilon}$, where $|\boldsymbol{\epsilon}|$ is assumed to be relatively small compared to unity.

With no loss in generality, we set the reference laboratory axes to be aligned with the crystal axes, *i.e.* $\mathbf{X}_1 = \mathbf{s}$ and $\mathbf{X}_2 = \mathbf{m}$. Figure 2 shows the geometry within the plane defined by $\mathbf{s}$ and $\mathbf{m}$. The angle between $\mathbf{n}$ and $\mathbf{s}$ is θ. Therefore we have

$$\mathbf{s} = \begin{pmatrix} 1 \\ 0 \end{pmatrix}, \quad \mathbf{m} = \begin{pmatrix} 0 \\ 1 \end{pmatrix}, \quad \text{and} \quad \mathbf{n} = \begin{pmatrix} cos\theta \\ sin\theta \end{pmatrix}. \tag{11}$$

There are two types of important imperfections that can induce kinking (see Figure 2): i) the loading axis tilt angle η, and ii) the local imperfection tilt angle η'. Both η and η' are taken to be quite small.

Now take that the compression axis is along the vertical axis $\mathbf{X}_1'$, then the kinking condition (10) becomes

$$-h - (C_{22} - \frac{C_{12}^2}{C_{11}})sin^2\theta - \sigma cos2\eta = 0\,, \tag{12}$$

where $C_{11} = L_{1111}$, $C_{22} = L_{2222}$, $C_{12} = L_{1122} = L_{2211}$, η is the loading axis tilt angle and σ is the uniaxial compression stress along the vertical $\mathbf{X}_1'$ axis (not $\mathbf{X}_1$ axis). Note that σ is negative when the composite is under compression.

Results

Case Studies and the Calculations of Kink Band Angle

Accurate predictions for kink band angles have been difficult to obtain within the available theories in the literature (see *e.g.* Budiansky and Fleck [1]). Here we will apply our model to predict kink band angles, and compare theoretical results with available experimental data.

Write h_m and τ_Y^m as the plastic shear strain hardening moduli and the shear yielding stress of the matrix respectively, for typical structural fiber composites with ductile matrix, we have $h_m \leq \mathcal{O}(\tau_Y^m)$ [2, 6, 21]. With composite shear strain hardening $h \approx h_m/(1 - V_f)$ and composite shear resistance $\tau_Y \approx \tau_Y^m/(1 - V_f)$, where V_f is the volume percentage of the fibers, we obtain $h \leq \mathcal{O}(\tau_Y)$. At the initial yielding, the composite yield stress $\sigma_Y = -\tau_Y/\bar{\phi}$ ($\bar{\phi}$ is usually less than 5^o), so that $\tau_Y \leq \mathcal{O}(0.1|\sigma_Y|)$. Therefore, we have

$$h \leq \mathcal{O}(0.1|\sigma_Y|).$$

Now, when η is small (about 2-4^o), our kinking condition (12) can be used to predict kink band angles, *i.e.*

$$\theta = \pm arc\,sin\sqrt{\frac{-\sigma - h}{C_{22} - C_{12}^2/C_{11}}} \approx \pm arc\,sin\sqrt{\frac{-\sigma}{C_{22} - C_{12}^2/C_{11}}}\,. \tag{13}$$

The results of the three case studies are summarized in Table 1, where the 5 independent elastic constants in fiber composites are denoted as axial Young's modulus E_A, transverse Young's modulus E_T, axial shear modulus G_A, major Poisson's ratio ν_A, and minor Poisson's ratio ν_T. We have found, as shown in

TABLE 1
Summary of the Three Case Studies

	Case #1 AS4/PEEK	Case #2 Carbon/PEEK	Case #3 Graphite/Epoxy
E_A (GPa)	*128	†220	‡206.90
E_T (GPa)	*10.57	†7	‡5.17
G_T (GPa)	*5.79	†4	‡2.59
ν_A	*0.3	†0.2	‡0.25
ν_T	*0.3	†0.25	‡0.25
C_{11} (GPa)	130.78	220.75	207.765
C_{22} (GPa)	11.78	7.483	5.529
C_{12} (GPa)	4.63	1.873	1.731
σ_C (MPa)	*1000 (Ring)	—	‡173 (Initiation)
Kink Angle (Experimental)	*15°	—	‡9°
Kink Angle (Theory%)	16.1°	—	10.2°
σ_C (MPa)	*1100 (Rod)	†1000 (Final)	‡202 (Final)
Kink Angle (Experimental)	*16.5°	†22°	‡12°
Kink Angle (Theory%)	17.9°	21.5°	11.0°

* Data from Kyriakides *et al.* [2].
† Data from Moran *et al.* [6] and Liu and Shih [18].
‡ Data from Waas *et al.* [19].
% Calculated using equation (13).

Table 1, that the critical kinking condition (12) or (13) is in excellent agreement with experimental data for fiber reinforced polymeric (ductile) matrix composites (within 2° for all three cases studied).

Critical Loading Stress σ_C and Yield Stress σ_Y

When the only non-zero stress component in (X_1', X_2') coordinate system is $\sigma_{11} = \sigma$, the the yield criterion becomes

$$\sigma_Y = -\frac{\tau_Y}{\bar{\phi}}, \tag{14}$$

where σ_Y is the yield stress of the composite and $\bar{\phi} = \eta + \eta'$ is the total imperfection tilt angle. It is experimentally verified that, when the compressive stress reaches the yield stress σ_Y obtained by (14), the kink band forms (see *e.g.* Budiansky [5], Jelf and Fleck [3], Kyriakides, Arseculeratne, Perry and Liechti [2], and Moran, Liu and Shih [6]).

Why can the composite yield stress be used as the critical loading stress for kink band formation?

First of all, it shall be stressed that, for the critical kinking condition (12) or (13) to be valid, the composite material must be in the plastic range. In another words, the initial yielding stress is the earliest possible kinking stress. With this in mind, we now take a closer look at the critical kinking condition (12).

Note that usually for fiber reinforced polymeric composites $E_T \ll E_A$, we have

$$C_{11} \approx E_A, \quad C_{22} \approx E_T, \quad \text{and} \quad C_{12} \approx \frac{\nu_A E_T}{1 - \nu_T}. \tag{15}$$

For the convenience, η is assumed to be very small, and (15) is substituted into (12). After rearrangement, we reduce (12) to a simple form, *viz.*

$$sin^2\theta = \frac{-\sigma - h}{E_T\left[1 - \left(\frac{\nu_A}{1-\nu_T}\right)^2\right]}. \tag{16}$$

Note that for typical structural fiber composites with ductile matrix $E_T \geq \mathcal{O}(10|\sigma|)$ (see Table 1), $\left[1-\left(\frac{\nu_A}{1-\nu_T}\right)^2\right] = \mathcal{O}(1)$, and $h \leq \mathcal{O}(0.1|\sigma|)$ at the initial yielding, we have

$$0 < \frac{-\sigma_Y - h}{E_T\left[1-\left(\frac{\nu_A}{1-\nu_T}\right)^2\right]} \leq \mathcal{O}(0.1)\,,$$

for compressive loading ($\sigma_Y < 0$). This means that there are *always* valid solutions for the kinking condition (16) or (12) at the initial yielding. Therefore, for a ductile matrix fiber composite under uniaxial compression, it is concluded that the critical kinking stress (σ_C) should be the same as the initial yield stress (σ_Y), *i.e.*

$$\sigma_C = \sigma_Y\,. \tag{17}$$

This provides some justification for why the yield criterion can be used to predict the critical stress for kink band formation.

Discussion

For a polymeric matrix fiber reinforced composite, a typical plot of shear stress vs. shear strain along the fiber direction is shown in Figure 3(a). An often used simple model for the shear stress vs. shear strain response is shown in Figure 3(b). A distinctive locking stage will be achieved after certain shear strain γ_H with the hardening being represented by H. Usually $\gamma_H > 0.5$. As discussed by Moran *et al.* [6], the deformation of $\gamma > \gamma_H$ (with hardening H) may be related to the kink band broadening as well as the load for steady state kinking.

Around the 'yield point' (see enlarged part shown in Figure 3(a)), $\partial\tau/\partial\gamma$ drops from some number of order G_T (about $0.4E_T$) to a fairly low value ($h \ll |\sigma_Y|$). From (13), it is clear that, as hardening ($h > 0$) decreases, the kink angle θ increases. It is therefore expected that, a kink band may initiate at an angle much shallower than the fully developed kink band angle, while the compressive stress may be only a little less than the peak (critical) stress. This phenomenon was also experimentally observed by Waas *et al.* [19] and Moran *et al.* [6].

The bifurcation analysis presented in this paper has predicted very good results for the kink band angles as compared with experiments. Noting that the experimental measured kink band angles are measured well after the bifurcation point, a possible explanation is that there is little additional rotation after the load drop. A full boundary value solution may be needed to find out underlying mechanisms, which will be dealt with in later efforts.

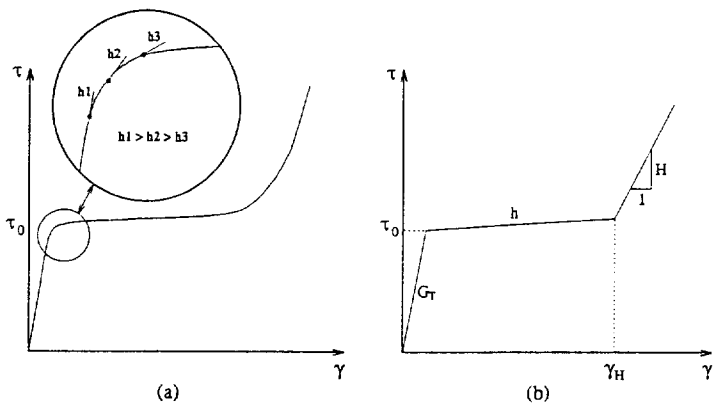

Figure 3. (a) A typical shear stress vs. shear strain curve along the fiber direction for a polymeric matric fiber reinforced composite. (b) An often used simple model for the shear stress vs. shear strain response for the composite material.

Conclusions

An elasto-plastic, finite strain, simple slip model is applied to study the critical conditions (*i.e.* the critical load and the kink band angle) for kink band formation for fiber composites under compressive loading. Orientation dependent mechanical behavior of fiber composites is modeled using simple slip along fiber direction, and elastic anisotropy of fiber composite is rigorously accounted for. To summarize the results presented in this paper, it is concluded that:

1) A closed form critical condition of the kink band formation for ductile matrix fiber composite, *viz.* equation (12), is derived.

2) The kink band angle can be computed using (12) or (13). Excellent agreement is found between theoretical predictions and available experiments (within 2^o for all three cases studied here).

3) Within our model framework, it is demonstrated that, for ductile matrix fiber composites under uniaxial compression, the critical loading stress σ_C should be the same as the composite yielding stress σ_Y, *i.e.*

$$\sigma_C = \sigma_Y \ .$$

This explains the experimentally verified fact that, the yield criterion (*e.g.* the resolved shear stress along fiber direction reaches a critical value) can be used to obtain the critical stress σ_C for kink band formation.

Acknowledgment

The authors acknowledge helpful discussions with Prof. T. H. Hao and Prof. Said Ahzi during the course of this study.

References

[1] B. Budiansky and N. A. Fleck, *J. Mech. Phys. Solids*, **41** (1993) 183-211.
[2] S. Kyriakides, R. Arseculeratne, E. J. Perry and K. M. Liechti, *Int. J. Solids Structures*, **32** (1995) 689-738.
[3] P. M. Jelf and N. A. Fleck, *J. Composite Materials*, **18** (1992) 2706-2721.
[4] A. S. Argon, *Treatise of Materials Science and Technology* (Vol. 1, Academic Press, New York, 1972), 79-114.
[5] B. Budiansky, *Computers Struc.*, **16** (1983) 3-12.
[6] P. M. Moran, X. H. Liu and C. F. Shih, *Acta Metall.*, **43** (1995) 2943-2958.
[7] R. Hill and J. R. Rice, *J. Mech. Phys. Solids*, **20** (1972) 401-413.
[8] R. J. Asaro and J. R. Rice, *J. Mech. Phys. Solids*, **25** (1977) 309-338.
[9] R. J. Asaro, *Acta metall.*, **27** (1979) 445-453.
[10] G. I. Taylor, in J. M. Lessels (ed.), *Stephen Timoshenko 60th Anniversary Volume* (Macmillan, New York, 1938), 218.
[11] D. Peirce, R. J. Asaro and A. Needleman, *Acta metall.*, **30** (1982) 1087-1119.
[12] D. Peirce, R. J. Asaro and A. Needleman, *Acta metall.*, **31** (1983) 1951-1976.
[13] M. Dao and R. J. Asaro, *Mater. Sci. Eng. A*, **170** (1993) 143-160.
[14] M. Dao and R. J. Asaro, *Scripta metall.*, **30** (1994) 791-796.
[15] M. Dao and R. J. Asaro, *Mechanics of Materials*, submitted for publication.
[16] M. Dao and R. J. Asaro, *Mechanics of Materials*, submitted for publication.
[17] R. Hill, *J. Mech. Phys. Solids*, **10** (1962) 1-16.
[18] X. H. Liu and C. F. Shih, manuscript in preparation.
[19] A. M. Waas, C. D. Babcock, Jr. and W. G. Knauss, *Int. J. Solids Structures*, **26** (1990) 1071-1098.
[20] R. M. Jones, *Mechanics of Composite Materials* (Scripta Book Co., Washington, 1975), 70.
[21] R. Jones, *Composite Structures*, **30** (1995) 193-199.